Proceedings of the
10th Graz Brain-Computer Interface Conference 2026
10.3217/978-3-99161-093-9-010

Resting-State EEG Predictors for BCI Performance: A Scoping Review

T. Settgast[1], R. Patel[2], A. Kübler[1]

[1] Institute of Psychology, Section Intervention Psychology, Julius-Maximilians-Universität Würzburg, Würzburg, Germany

[2] Electronic and Electrical Engineering, University College London, London, United Kingdom

E-mail: tomko.settgast@uni-wuerzburg.de

ABSTRACT: This scoping review summarizes studies investigating the association between resting-state EEG and subsequent BCI performance. Following PRISMA-ScR guidelines, we systematically mapped the literature to provide a comprehensive overview. We discuss the results within the context of BCI performance prediction, emphasizing the importance of resting-state brain activity, particularly for patient-centered research.

INTRODUCTION

Resting-state brain activity influences subsequent stimulus-induced activity, and vice versa [1,2]. Additionally, resting-state brain activity relates to subsequent task performance [3,4]. Therefore, resting-state brain activity contains valuable information about a subject's cognitive state [5] that is relevant to stimulus processing and task performance. Recently, there have been calls to recognize this user's state [6] and to use resting-state dynamics to optimize brain-computer interface (BCI) use [7].
This scoping review maps experimental studies relating resting-state electroencephalography (EEG) to subsequent BCI performance, discussing these results in the broader context of BCI performance predictors. We emphasize the potential of resting-state brain activity for BCI use, particularly for patient groups who could greatly benefit from BCIs, such as those in the locked-in (LIS) or complete locked-in state (CLIS) [8].

MATERIALS AND METHODS

This review follows the *PRISMA-ScR* guidelines [9]. We searched *Web of Science* and *IEEE Xplore* for experimental studies linking resting-state EEG to subsequent BCI performance (last search: October 16, 2025), using the search query term "(BCI OR brain-computer interface OR brain-machine interface OR direct neural interface OR thought-translation device OR speller) AND (correlate OR predictor) AND resting-state", and restricted the search to the title, abstract, and keywords. The review protocol was not pre-registered. Inclusion was restricted to active BCI paradigms; passive BCIs were excluded. Resting-state was defined as a passive acquisition state, with the eyes open or closed [5]. To ensure signal stability [10], we excluded studies with recordings shorter than 30 seconds, e.g., pre-stimulus activity, and (concatenated) between/inter-trial resting epochs. We also excluded studies that used *rest* merely as a control condition, as well as those that made resting-state recordings exclusively after BCI use or between BCI blocks. Records were divided between two authors (TS and RP) for screening (no overlap). Uncertain cases were discussed jointly. Data extraction included resting-state EEG feature(s), the resting-state protocol, the BCI paradigm, participant demographics, and BCI performance associations (see Tab. 1).

RESULTS

Database searches identified 372 records (IEEE Xplore: N = 86; Web of Science: N = 286). Seven papers were added manually. Four of these papers were known to the authors but were not retrieved by the screening strategy. The other three were found through reference checking. After screening and an eligibility assessment (see Fig. 1 for details), 23 studies were included in the review (see Tab. 1). One study that was initially added on behalf of the authors was deemed ineligible after a thorough assessment.

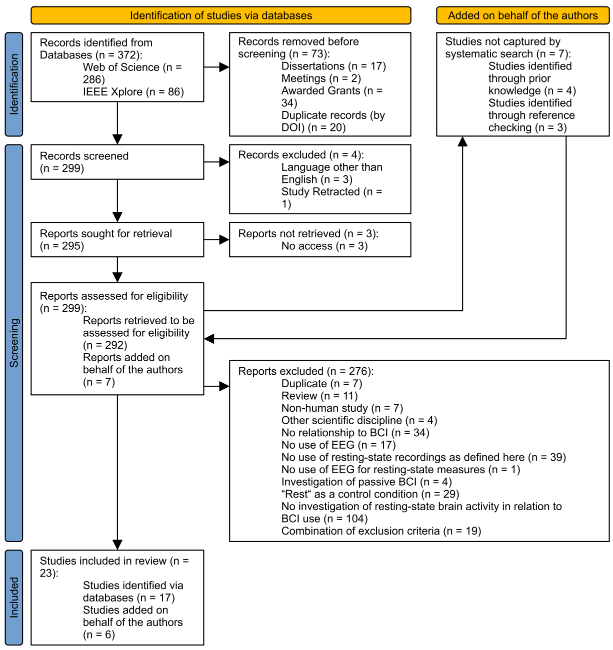

Figure 1: PRISMA flowchart of the study selection process, following the structure suggested for PRISMA reviews [11].

10.3217/978-3-99161-093-9-010

Overview

Table 1: **Overview of reported associations between resting-state EEG features and BCI performance**.

Ref.	Resting-State EEG Feature(s)	Resting-State Protocol	BCI Paradigm	Participants	Results (Association with BCI Performance)
[12]	*SMR predictor*	EO/EC (10x15s); task (EO): fix. moving shapes. Anal.: concatenated EO.	SMR (MI) BCI	N = 148/168 (H)	*SMR predictor* ↑ (r = .53; r = .66 without outlier).
[13]	RPL of canonical frequency bands (except δ) & *PPfactor*	"Non-task related state", EO; task: mind-wandering, think about nothing. Duration: NR.	MI BCI	N = 52 (H) + N = 9 (H), Data: [14]	High performer: low θ (4-8 Hz) & high α (8-13 Hz) RPL. *PPfactor* ↑ (r = .59; r = .70 without outlier).
[15]	*SMR predictor*	EO/EC (10x15s); task: relax. Anal.: concatenated EO.	SMR (MI) BCI	N = 80 (H)	*SMR predictor* ↑ (r = .53; r = .61 without outlier; ~28% variance explained).
[16]	PSD (δ, θ, α, β) in four ROI	5 min EO, task: fix.dot, stay relaxed. Anal.: central 4 min.	"Visuo-mental" BCI (3 protocols)	N = 5 ALS patients + N = 6 (H)	Stepwise MLR: Temporo-parietal δ (1-3 Hz) power identified as a negative predictor for performance. Model includes H & ALS patients.
[17]	Relative PSD & IAF	EO (5x6s); task: fix. non-flickering LEDs. Anal.: concatenated EO ("baseline resting state").	SSVEP BCI (4 classes)	N = 18 (H)	***ACL***: relative "thetaHigh" (6.5-7.5 Hz) ↑ (r = .47), relative "betaMid" (18-24Hz) ↓ (r = -.53 without outlier) at Oz. IAF ↑ (r = .58 without outlier). ***Top. Freq.***: relative "betaMid" ↑ at F3 (r = .48).
[18]	Coupling strength in motor network (EffC via DCM)	1 min EO; task: gaze at center. 2 sessions on different days.	MI BCI	N = 54 (H), Data: [19]	High performer: stronger SMA → DLPFC coupling. SMA → DLPFC coupling ↑ (Session 1: r = .54; Session 2: r = .42) & predicts MI BCI performance.
[20]	Network efficiency (Graph Theory Metrics: CC, CPL, GE & LE) & *NEI* derived from FC/EffC	1 min EO; task (Dataset 2): gaze at center. Dataset 2: 2 sessions on different days.	MI BCI	N = 52 (H), Data: [21] + N = 54 (H), Data: [19]	High performer: higher network efficiency (eps. α-band: 8-13 Hz). NEI (COH/PLV) ↑ (r = .37/.35 without outlier) & predicts MI performance (*RMSE*: 13.31%/13.37%).
[22]	Spectral features (C3/C4): fmax, at fmax: PSD/noise (1/f) fit, *SMR Predictor*	EO/EC (10x15s); task: relax. Anal.: concatenated EO.	SMR (MI) BCI	N = 78/80 (H), Data: [15]	*SMR predictor* ↑ (r = .53; ~28% variance explained). Further corr. at C3/C4: noise/PSD fit, fmax. Corr. from average (C3 + C4) > single channels.
[23]	*Criticality-related measures* (1-40 Hz, scalp-wide average): PLE, LZC	EO/EC (139s each), task: fix. cross, stay relaxed. Anal.: EO (before BCI, 130s).	Visual P300 BCI speller.	N = 55 (H), Data: [24]	LZC ↑ (r = .38), PLE ↓ (r = -.34).
[25]	*Criticality-related measures* (1-40 Hz, scalp-wide average): PLE, LZC	LIS-ALS: 1-2 min, EO, no task. Anal.: central 110s. H: EO/EC (139s each), task: fix. cross, stay relaxed. Anal.: EO (before BCI, central 110s).	LIS-ALS: vibrotactile P300 BCI. H: visual P300 BCI speller.	N = 1 (LIS-ALS patient, N = 10 sessions), Data: [26] + N = 55 (H), Data: [24]	LIS-ALS (longitudinal): PLE ↑ (r = .76), LZC ↓ (r = -.75). H: Ø (ceiling effects), but opposite trends.
[27]	PSD, functional connectivity (PLV) in four ROIs (Frontal, Central, Parietal, Occipital)	4 min EC, no task.	Visual P300 BCI speller	N = 8 (H)	Frontal δ (0.5-4 Hz) power ↓ (r = -.94), frontal δ connectivity ↓ (r = -.77 to -.88), α (8-12 Hz) connectivity ↓ (Frontal-Central; r = -.73), γ (30-45 Hz) connectivity ↑ (Frontal-Occipital; r = .77).
[28]	PSD, RPL	EO/EC (3 min each), task: fix. cross.	MI BCI (unilateral)	N = 26 (H)	α (8-13 Hz) PSD/RPL ↓ (max. correlation with PSD at AF8: r = -.44), β (13-30 Hz) PSD/RPL ↑ (max correlation with PSD at Fp1: r = .65). Significant corr.: EO > EC.
[29]	Weighted PDFs derived from PSD	EO/EC (10x15s); task: relax. Anal.: EO + EC.	SMR (MI) BCI	N = 80/83 (H), Data: [15]	High performer: visible peaks in μ- (8-12 Hz) and β- (16-22 Hz) bands in PDFs. Linear regression based on these clusters predicts performance (r = .58) using only C3, Cz, and C4.
[30]	At Oz: *Alpha predictor* & slope of the 1/f PSD component (referred to as "lambda")	EO/EC (2 min each, once before & once after BCI), task: fix. cross. Anal.: EO (before BCI).	c-VEP BCI	N = 26 (H)	Ø. *Alpha* predictor **non-significant** trend ↓ (r = -.18; r = -.29 without outlier), & slope of the 1/f PSD component **non-significant** trend ↑ (r = .13).
[31]	*SMR predictor*, *PPfactor* & spectral peak metrics (sum of the number of peaks & variance of the peak frequency) at C3/C4	EO/EC (3 min each), task: relax, fix. cross. Anal.: EO (2 min extracted).	MI BCI	N = 85/87 (H), Data: [32]	*SMR predictor* ↑ (ρ = .49), variance of the μ-band peak frequency ↓ (ρ = -.33), number of peaks ↑ (ρ = .24), *PPfactor Ø*.
[33]	*μ- & β-band predictor*, spectral peak dynamics in μ- (5-15 Hz) & β-band (15-25 Hz) (C3/C4): peak width/frequency, num. of peaks, (temporal) variance of amplitude/frequencies of μ-band peak (width)	3 min EO, task: relax. Anal.: 2 min extracted.	MI BCI	N = 56/59 (H), Data: [34]	*μ-band predictor* ↑ (r = .43), mean (C3 & C4) μ-band peak width ↑ (r = .27), number of peaks ↑ (r = .35), temporal variance of the μ-band peak frequency ↓ (r = -.48). Combined features predict performance (*MAE* = 12.43%).
[35]	Relative IAB amplitude at Oz	EO/EC (1 min each), no task. Anal.: EO.	SSVEP (ten classes)	N = 33 (H)	IAB amplitude ↓ (SNR: r = -.42; classification accuracy: r = -.58). Neurofeedback-based downregulation of IAB improves performance.
[36]	RPL & non-linear metrics (LZC & PSE) (frequency-band- and channel-wise)	EO/EC (1 min each), no task. Anal.: EO + EC (individually).	MI BCI	N = 105/109 (H), Data: [37,38]	Strongest correlations in α-band (8-13 Hz; EO). At C4: RPL ↑ (r = .50), PSE ↓ (r = -.53), LZC ↓ (r = -.46). Combined features classify high/low performer (84.05% accuracy).
[39]	Normalized occipital "alphaLow" (7.5-9 Hz) & "alphaHigh" (9-12.5 Hz) band power	1 min, no task. Anal.: last 45s. No information if eyes open/closed.	SSVEP-based QWERTY speller (30 classes)	N = 26 (H)	Correlation depends on SSVEP-stimulation frequency. Low-frequency SSVEP: "alphaLow" ↓ (r = -.62), "alphaHigh" ↓ (r = -.52).
[40]	Coupling strength in DMN (EffC via DCM)	1 min EO, no task.	MI BCI	N = 52 (H), Data: [21]	High performer: weaker lLP-rLP coupling strength. lLP-rLP coupling strength ↓ (r = -.37).
[41]	Mean FC (COH) & network topology (CC & CPL) (five	2 min EC, no task. Anal.: seven	SSVEP experiment (BCI	N = 12 (H)	Significant corr. for freq.-specific RS features (excl. 10 Hz) & averages across frequencies. Corr. between averaged RS features and averaged SNR: mean FC ↓ (r = -.80), CC ↓ (r = -.78), CPL ↑ (r = .85). Corr. with

 10.3217/978-3-99161-093-9-010

	frequencies: 7.5, 10, 12, 15, 20 Hz).	concatenated artifact-free 10s epochs.	equivalent) (5 classes)		classification accuracy: SNR ↑ (r = .67), relative "alphaHigh" (9-12.5 Hz) ↓ (r = -.64). Best model (normalized CC and normalized reciprocal CPL): R^2 = .76.
[42]	Mean SE based on relative PSD (0.5-14 Hz), *SMR predictor* & *ATR predictor*	EO/EC (2 min each, order randomized), no task. Anal.: central 100s.	SMR (MI)	N = 40 (H) (N = 26 re-tested in 2nd session)	Mean SE ↑ (maximum correlations at C3, EC): Session 1: r = .61; Session 2: r = .70. Pooled dataset (N = 66 sessions): mean SE (C3, EC) ↑ (r = .65), outperforming *ATR predictor* (FC3, EC; r = .51) and *SMR predictor* (C4, EO; r = .29). LDA classifier (mean SE) predicts aptitude with 75% (Session 1) and 89% (Session 2) accuracy.
[43]	Mean FC, node degree, edge strength, network efficiency (CC, CPL, LE, GE) based on COH & PLI (4-14 Hz)	EO/EC (2 min each, order randomized), no task. Anal.: central 100s.	SMR (MI)	N = 40 (H) (N = 26 re-tested in 2nd session), Data: [42]	Network efficiency (higher CC, LE, GE; lower CPL) ↑, mean FC ↑, node degree ↑, edge strength ↑. COH-based metrics outperform PLI-based metrics. Session-1 RS network efficiency (COH) predicts Session-2 classification accuracy (r = .61, *RMSE* = 12.2%).

*Notes: **Ref.**: numerical reference. **Resting-State Protocol**: Anal. = analysis based on. **Participants**: H = healthy participants; ALS = amyotrophic lateral sclerosis; LIS = locked-in state. **Results**: ↑/↓ = positive/negative correlation; Ø = no correlation. All reported correlations refer to correlations with performance metrics. Highlighted in light green: identified through reference checking. Highlighted in light purple: identified through prior knowledge but not retrieved by screening strategy. **Abbreviations**: ACL: assisted closed-loop protocol; CC: clustering coefficient; CPL: characteristic path length; COH: coherence; DCM: dynamic causal modeling; DLPFC: dorsolateral prefrontal cortex; EO/EC: eyes open/closed; DMN: default-mode network; EffC: effective connectivity; fmax: frequency maximizing difference between modeled PSD and noise fit; FC: functional connectivity; GE: global efficiency; IAF/IAB: individual alpha frequency/band; LE: local efficiency; ILP: left lateral parietal area; LZC: Lempel-Ziv complexity; MAE: mean absolute error; MLR: multivariate linear regression; NEI: network efficiency indicator; NR: not reported; PDF: probability density function; PLE: power-law exponent; PLI/PLV: phase-locking index/value; PPfactor: performance potential factor; (P)SE: (power) spectral entropy; RMSE: root mean square error; rLP: right lateral parietal area; RPL: relative power level; ROI: sensor-based regions of interest; SMA: supplementary motor area; STR: strength; Top. Freq.: protocol using top frequencies.*

Of 23 eligible studies (six conference proceedings [23,25,27,31,33,40], 17 journal articles; 2010-2025), 14 focused on motor imagery (MI) BCIs [12,13,15,18,20,22,28,29,31,33,36,40,42,43], four on steady-state visually evoked potential (SSVEP)-based BCIs [17,35,39,41], and three on P300-based BCIs [23,25,27]. Single studies investigated a BCI using code-modulated visual evoked potentials (c-VEP) [30], and “visuo-mental” BCI protocols combining a P300 speller and an arithmetic task [16]. Participants were predominantly healthy (N = 8 to 148); only two studies included patients with amyotrophic lateral sclerosis (ALS) [16,25] – one of whom was in LIS [25].

Resting-State EEG Predictors Detailed associations between resting-state EEG features and BCI performance are provided in Tab. 1.

For MI BCIs, the *SMR predictor* – reflecting the mean peak amplitude difference between a fitted power spectral density (PSD) and a fitted 1/f noise spectrum at Laplacian channels C3 and C4 [15] – showed consistent positive correlations with performance [12,15,22,31,42]. Another C3/C4-based metric, the *performance potential factor* (*PPfactor*) [13], showed less consistency; a recent replication attempt [31] failed to confirm the originally reported positive correlation. In general, channels C3 and C4 were repeatedly identified as optimal recording sites for correlations with subsequent BCI performance across EEG features [22,29,33,36,42]. For example, the number of peaks in the PSD and the dynamics of the μ-frequency band peaks have repeatedly been shown to correlate with MI BCI performance [31,33]. More generally, the prominent presence of μ- and β-frequency band activity in the PSD appears to be associated with MI BCI performance. For example, Suk et al. [29] were able to cluster high and low performers based on the visibility of peaks in the μ- and β-frequency bands in the subjects’ probability density functions, and, recently, Sonntag et al. [28] showed positive correlations between absolute and relative β-frequency band power and accuracy.

Associations with resting-state α-frequency band activity appear to be paradigm-specific. For MI BCIs, high performance generally relates to high α-frequency band relative power level (RPL) [13,36] alongside low θ-frequency band RPL [13], though the inverse pattern was also observed [28]. In contrast, for SSVEP-based BCIs, (parieto-)occipital resting-state α-frequency band activity consistently correlates negatively with subsequent performance [35,39,41]. Wan et al. [35] even demonstrated that decreasing the individual α-band amplitude with neurofeedback improved performance with a SSVEP-based BCI.

Negative associations were observed between resting-state δ-frequency band power and BCI performance. In healthy participants, it negatively correlated with subsequent P300-based speller performance [27]. Similarly, temporo-parietal resting-state δ-frequency band power was retained as a significant negative predictor in a multivariate linear regression model for predicting visuo-mental BCI performance [16]. The model was trained with data from ALS patients and healthy participants.

Paradigm-specific patterns also emerged for connectivity and network features. Across studies, higher network efficiency at rest was associated with better MI BCI performance. This was demonstrated in a 4-14 Hz frequency band [43] and the α-frequency band [20]. Conversely, for SSVEP-based BCIs, mean functional connectivity and greater network efficiency across frequencies were negatively correlated with the SSVEP signal-to-noise ratio [41].

Non-linear features yielded inconclusive results. Spectral entropy exhibited both positive [42] and negative correlations [36] with MI BCI performance – the latter accompanied by negative correlations between performance and Lempel-Ziv complexity (LZC) [36] – potentially depending on the frequency bands used and eye closure during rest. Regarding P300-based BCIs, scalp-wide average broadband (1-40 Hz) LZC at rest was positively correlated with subsequent BCI performance in healthy participants [23], but negatively in a LIS-ALS patient [25].

Similarly, the slope of the 1/f PSD component exhibited inverted patterns. While healthy participants performed better with a flatter slope (i.e., smaller power-law

 10.3217/978-3-99161-093-9-010

exponents) [23], performance in a LIS-ALS patient increased with a steeper slope [25]. Thielen [30] investigated this feature with regard to c-VEP-based BCI use. The study yielded a positive – albeit non-significant – correlation at electrode Oz, suggesting that a steeper slope at rest is related to better BCI performance. Lastly, Sanneli et al. [22] reported a correlation with the 1/f "noise" at rest and BCI performance at electrode C3. However, the 1/f "noise" was investigated only at the frequency that maximized the difference between the fitted PSD and the fitted 1/f spectrum at the Laplacian electrodes C3 and C4. Therefore, a direct comparison to studies investigating the 1/f slope [23,25,30] is impossible.

DISCUSSION

While psychological [44–46] and neurophysiological [47] factors are known to influence BCI performance, resting-state EEG prior to BCI use has largely been neglected in patient-centered research. This scoping review demonstrates that resting-state EEG contains valuable information about subsequent BCI performance, yet, only two of the 23 included studies examined patients [16,25].

Despite most studies reporting correlations rather than *predictions*, the temporal precedence of the resting-state EEG before BCI operation supports their interpretation as candidate predictors.

Crucially, resting-state EEG predictors appear paradigm-specific. For MI BCIs, results are consistent for the *SMR predictor* [12,15,22,31,42], as well as for higher mean functional connectivity, and network efficiency [20,43]. Furthermore, μ- and β-frequency band activity at rest appears to be important for subsequent MI BCI performance [28,29,31,33], as is information from electrodes C3 and C4 [12,13,15,22,29,31,33,36,42].

Conversely, performance with SSVEP-based BCIs shows inverted connectivity and network feature patterns. Mean functional connectivity and network efficiency metrics were negatively correlated with performance [41]. More importantly, α-frequency band activity appears to be particularly relevant for SSVEP-based BCI use. Particularly at (parieto-)occipital electrodes, α-frequency band activity showed consistent negative correlations with performance across studies [35,39,41]. These results suggest that an *optimal* user state is specific to the BCI paradigm. Although this heterogeneity prevents a meta-analysis across all featured studies, the consistent association between the SMR predictor and MI BCI performance [12,15,22,31,42] may justify a focused meta-analysis on this subsample in the future.

The transferability of predictors to patient samples also appears to be feature-dependent. For example, Borgheai et al. [16] found that resting-state δ-frequency band power remained a negative predictor in a regression model for predicting BCI performance involving data from healthy participants and ALS patients. However, LZC and the slope of the 1/f PSD component exhibited inverted correlation patterns in a LIS-ALS patient [25] compared to healthy participants [23]. We hypothesize that the *brain criticality hypothesis* [48] could reconcile these conflicting results, given that LZC and the 1/f slope are both considered *criticality-related measures* [49]. The brain criticality hypothesis proposes a nonlinear relationship between information processing capacity and proximity to the point of criticality [48,50]. While healthy participants with brain activity close to criticality [51] are likely to approach the point of criticality with a flatter 1/f slope and increasing LZC values, the LIS-ALS patient may demonstrate a shift to supercriticality [23,25] due to ALS-related hyperexcitability [52] and the connection between hyperexcitability and supercritical dynamics [53]. This could help to explain the inverted correlation patterns observed for healthy controls and the LIS-ALS patient [23,25], suggesting that BCI performance predictors may be transferable to clinical populations when the underlying pathophysiology of the clinical sample is considered.

The 1/f slope emerges as a promising marker of user state fluctuations. Not only does it track changes in the ratio of excitatory to inhibitory synaptic activity [54], which, for its part, is related to changes in criticality [53], but it appears to change globally across the scalp – reducing the need for high-density electrode coverage [55]. However, conflicting results between Settgast and Kübler [23] and Thielen [30] call for further investigation. It is unclear whether patterns observed for P300-based BCIs [23,25] can easily be transferred to another BCI paradigm and whether a single electrode can adequately reflect the global change in the 1/f slope across the scalp.

This review emphasizes that ignoring systematic patterns between resting-state EEG and BCI performance can result in explainable variance being overlooked. This seems to be particularly significant for potential end-user groups, such as ALS patients [56], and is likely to increase with the consciousness fluctuations observed in CLIS [57,58]. To focus efforts on features related to promising *Windows of Consciousness* [59], systematic investigations in potential end-user groups are essential. To facilitate future systematic reviews and potential meta-analyses, we strongly recommend recording resting-state brain activity before BCI use and systematically reporting the recording length, to avoid confusion with other resting epochs during the BCI use, as well as reporting the eye status (open vs. closed) during the recording.

CONCLUSION

This scoping review identified consistent, yet paradigm-specific, associations between resting-state EEG and BCI performance. One key finding indicates that potential predictors may not easily transfer to patient samples without considering the underlying pathophysiological processes. This overview can guide future studies investigating resting-state EEG predictors for BCI performance in potential end-user groups. It may also

 10.3217/978-3-99161-093-9-010

provide essential information for detecting *Windows of Consciousness* that allow for BCI-based communication, even for patients in CLIS.

REFERENCES

[1] Northoff G, Duncan NW, Hayes DJ. The brain and its resting state activity—Experimental and methodological implications. Prog Neurobiol 2010;92(4):593–600.
[2] Northoff G, Qin P, Nakao T. Rest-stimulus interaction in the brain: a review. Trends Neurosci 2010;33(6):277–84.
[3] Cross ZR, Chatburn A, Melberzs L, Temby P, Pomeroy D, Schlesewsky M, et al. Task-related, intrinsic oscillatory and aperiodic neural activity predict performance in naturalistic team-based training scenarios. Sci Rep 2022;12(1):16172.
[4] Xu L, Feng J, Yu L. Avalanche criticality in individuals, fluid intelligence, and working memory. Hum Brain Mapp 2022;43(8):2534–53.
[5] Finn ES. Is it time to put rest to rest? Trends Cogn Sci 2021;25(12):1021–32.
[6] Han Y, Ziebell P, Riccio A, Halder S. Two sides of the same coin: adaptation of BCIs to internal states with user-centered design and electrophysiological features. Brain-Comput Interfaces 2022;9(2):102–14.
[7] Nikulin V. Predicting task performance and brain responses with ongoing neural activity. 2022 10th Int. Winter Conf. Brain-Comput. Interface BCI, 2022, p. 1–2.
[8] Kübler A, Mattia D, Rupp R, Tangermann M. Facing the challenge: Bringing brain–computer interfaces to end-users. Artif Intell Med 2013;59(2):55–60.
[9] Tricco AC, Lillie E, Zarin W, O'Brien KK, Colquhoun H, Levac D, et al. PRISMA Extension for Scoping Reviews (PRISMA-ScR): Checklist and Explanation. Ann Intern Med 2018;169(7):467–73.
[10] Gudmundsson S, Runarsson TP, Sigurdsson S, Eiriksdottir G, Johnsen K. Reliability of quantitative EEG features. Clin Neurophysiol 2007;118(10):2162–71.
[11] Page MJ, McKenzie JE, Bossuyt PM, Boutron I, Hoffmann TC, Mulrow CD, et al. The PRISMA 2020 statement: an updated guideline for reporting systematic reviews. BMJ 2021;372:n71.
[12] Acqualagna L, Botrel L, Vidaurre C, Kübler A, Blankertz B. Large-Scale Assessment of a Fully Automatic Co-Adaptive Motor Imagery-Based Brain Computer Interface. PLOS ONE 2016;11(2):e0148886.
[13] Ahn M, Cho H, Ahn S, Jun SC. High theta and low alpha powers may be indicative of BCI-illiteracy in motor imagery. PLoS ONE 2013;8(11).
[14] Leeb R, Lee F, Keinrath C, Scherer R, Bischof H, Pfurtscheller G. Brain–Computer Communication: Motivation, Aim, and Impact of Exploring a Virtual Apartment. IEEE Trans Neural Syst Rehabil Eng 2007;15(4):473–82.
[15] Blankertz B, Sannelli C, Halder S, Hammer EM, Kübler A, Müller K-R, et al. Neurophysiological predictor of SMR-based BCI performance. NeuroImage 2010;51(4):1303–9.
[16] Borgheai SB, Zisk AH, McLinden J, Mcintyre J, Sadjadi R, Shahriari Y. Multimodal pre-screening can predict BCI performance variability: A novel subject-specific experimental scheme. Comput Biol Med 2024;168:107658.
[17] Fernandez-Vargas J, Pfaff HU, Rodriguez FB, Varona P. Assisted closed-loop optimization of SSVEP-BCI efficiency. Front Neural Circuits 2013;7.
[18] Lee M, Yoon J-G, Lee S-W. Predicting Motor Imagery Performance From Resting-State EEG Using Dynamic Causal Modeling. Front Hum Neurosci 2020;14.
[19] Lee M-H, Kwon O-Y, Kim Y-J, Kim H-K, Lee Y-E, Williamson J, et al. EEG dataset and OpenBMI toolbox for three BCI paradigms: an investigation into BCI illiteracy. GigaScience 2019;8(5):giz002.
[20] Park H, Jun SC. Connectivity study on resting-state EEG between motor imagery BCI-literate and BCI-illiterate groups. J Neural Eng 2024.
[21] Cho H, Ahn M, Ahn S, Kwon M, Jun SC. EEG datasets for motor imagery brain–computer interface. GigaScience 2017;6(7):gix034.
[22] Sannelli C, Vidaurre C, Müller K-R, Blankertz B. A large scale screening study with a SMR-based BCI: Categorization of BCI users and differences in their SMR activity. PLOS ONE 2019;14(1):e0207351.
[23] Settgast T, Kübler A. Resting-State Brain Criticality and Performance with P300-based BCIs. Proc. 9th Graz Brain-Comput. Interface Conf. 2024, Graz, Austria: Verlag der Technischen Universität Graz; 2024, p. 162–7.
[24] Won K, Kwon M, Ahn M, Jun SC. EEG Dataset for RSVP and P300 Speller Brain-Computer Interfaces. Sci Data 2022;9(1):388.
[25] Settgast T, Zilio F, Kübler A, Northoff G. Correlation between Neurophysiological Measures of Consciousness and BCI Performance in a Locked-in Patient. 2023 11th Int. Winter Conf. Brain-Comput. Interface BCI, 2023, p. 1–6.
[26] Ziebell P, Pfeiffer M, Tröger W, Halder S, Giesler T, Kübler A, et al. Persistent tactile P3 in long-term brain-computer interface home use by a patient in locked-in state 2024.
[27] Shin G-H, Lee M, Kim H-J, Lee S-W. Prediction of Event Related Potential Speller Performance Using Resting-State EEG. 2020 42nd Annu. Int. Conf. IEEE Eng. Med. Biol. Soc. EMBC, Montreal, QC, Canada: IEEE; 2020, p. 2973–6.
[28] Sonntag J, Yu L, Wang X, Schack T. Neurophysiological predictors of deep learning based unilateral upper limb motor imagery classification. Front Hum Neurosci 2025;19.
[29] Suk H-I, Fazli S, Mehnert J, Müller K-R, Lee S-W. Predicting BCI Subject Performance Using Probabilistic Spatio-Temporal Filters. PLOS ONE 2014;9(2):e87056.
[30] Thielen J. Addressing BCI inefficiency in c-VEP-based BCIs: A comprehensive study of neurophysiological predictors, binary stimulus sequences, and user comfort. Biomed Phys Eng Express 2025;11(4):045017.
[31] Trocellier D, N'Kaoua B, Lotte F. Validating neurophysiological predictors of BCI performance on a

10.3217/978-3-99161-093-9-010

large open source dataset. GBCIC 2024 - 9th Graz Brain-Comput. Interface Conf. 2024, Graz, Austria: 2024.

[32] Dreyer P, Roc A, Pillette L, Rimbert S, Lotte F. A large EEG database with users' profile information for motor imagery brain-computer interface research. Sci Data 2023;10(1):580.

[33] Tzdaka E, Benaroch C, Jeunet C, Lotte F. Assessing The Relevance Of Neurophysiological Patterns To Predict Motor Imagery-based BCI Users' Performance. 2020 IEEE Int. Conf. Syst. Man Cybern. SMC, 2020, p. 2490–5.

[34] Roc A, Pillette L, N'Kaoua B, Lotte F. Would Motor-Imagery based BCI user training benefit from more women experimenters? GBCIC2019 - 8th Graz Brain-Comput. Interface Conf. 2019, Graz, Austria: 2019.

[35] Wan F, da Cruz JN, Nan W, Wong CM, Vai MI, Rosa A. Alpha neurofeedback training improves SSVEP-based BCI performance. J Neural Eng 2016;13(3):036019.

[36] Wang K, Tian F, Xu M, Zhang S, Xu L, Ming D. Resting-State EEG in Alpha Rhythm May Be Indicative of the Performance of Motor Imagery-Based Brain–Computer Interface. Entropy 2022;24(11):1556.

[37] Goldberger AL, Amaral LAN, Glass L, Hausdorff JM, Ivanov PCh, Mark RG, et al. PhysioBank, PhysioToolkit, and PhysioNet. Circulation 2000;101(23):e215–20.

[38] Schalk G, McFarland DJ, Hinterberger T, Birbaumer N, Wolpaw JR. BCI2000: a general-purpose brain-computer interface (BCI) system. IEEE Trans Biomed Eng 2004;51(6):1034–43.

[39] Won D-O, Hwang H-J, Dähne S, Müller K-R, Lee S-W. Effect of higher frequency on the classification of steady-state visual evoked potentials. J Neural Eng 2015;13(1):016014.

[40] Yoon J-G, Lee M. Effective Correlates of Motor Imagery Performance based on Default Mode Network in Resting-State. 2020 8th Int. Winter Conf. Brain-Comput. Interface BCI, 2020, p. 1–5.

[41] Zhang Y, Xu P, Guo D, Yao D. Prediction of SSVEP-based BCI performance by the resting-state EEG network. J Neural Eng 2013;10(6):066017.

[42] Zhang R, Xu P, Chen R, Li F, Guo L, Li P, et al. Predicting Inter-session Performance of SMR-Based Brain–Computer Interface Using the Spectral Entropy of Resting-State EEG. Brain Topogr 2015;28(5):680–90.

[43] Zhang R, Yao D, Valdés-Sosa PA, Li F, Li P, Zhang T, et al. Efficient resting-state EEG network facilitates motor imagery performance. J Neural Eng 2015;12(6):066024.

[44] Geronimo A, Simmons Z, Schiff SJ. Performance predictors of brain-computer interfaces in patients with amyotrophic lateral sclerosis. J Neural Eng 2016;13(2).

[45] Riccio A, Simione L, Schettini F, Pizzimenti A, Inghilleri M, Olivetti Belardinelli M, et al. Attention and P300-based BCI performance in people with amyotrophic lateral sclerosis. Front Hum Neurosci 2013;7.

[46] Riccio A, Schettini F, Simione L, Pizzimenti A, Inghilleri M, Olivetti-Belardinelli M, et al. On the Relationship Between Attention Processing and P300-Based Brain Computer Interface Control in Amyotrophic Lateral Sclerosis. Front Hum Neurosci 2018;12(May):1–10.

[47] Halder S, Ruf CA, Furdea A, Pasqualotto E, De Massari D, van der Heiden L, et al. Prediction of P300 BCI Aptitude in Severe Motor Impairment. PLoS ONE 2013;8(10):e76148.

[48] O'Byrne J, Jerbi K. How critical is brain criticality? Trends Neurosci 2022;45(11):820–37.

[49] Maschke C, O'Byrne J, Colombo MA, Boly M, Gosseries O, Laureys S, et al. Critical dynamics in spontaneous EEG predict anesthetic-induced loss of consciousness and perturbational complexity. Commun Biol 2024;7(1):1–14.

[50] Müller PM, Miron G, Holtkamp M, Meisel C. Critical dynamics predicts cognitive performance and provides a common framework for heterogeneous mechanisms impacting cognition. Proc Natl Acad Sci 2025;122(14):e2417117122.

[51] Meisel C, Olbrich E, Shriki O, Achermann P. Fading Signatures of Critical Brain Dynamics during Sustained Wakefulness in Humans. J Neurosci 2013;33(44):17363–72.

[52] Gunes ZI, Kan VWY, Jiang S, Logunov E, Ye X, Liebscher S. Cortical Hyperexcitability in the Driver's Seat in ALS. Clin Transl Neurosci 2022;6(1):5.

[53] Javed E, Suárez-Méndez I, Susi G, Román JV, Palva JM, Maestú F, et al. A Shift Toward Supercritical Brain Dynamics Predicts Alzheimer's Disease Progression. J Neurosci 2025;45(9).

[54] Gao R, Peterson EJ, Voytek B. Inferring synaptic excitation/inhibition balance from field potentials. NeuroImage 2017;158:70–8.

[55] Hebron H, Stephan AM, Cataldi J, Siclari F. Aperiodic EEG Activity Provides a Linear, Bidirectional, and Spatially Uniform Marker of Subjective and Objective Vigilance in Humans, Both Within and Across States 2025:2025.08.30.673229.

[56] Marchetti M, Priftis K. Brain-computer interfaces in amyotrophic lateral sclerosis: A metanalysis. Clin Neurophysiol 2015;126(6):1255–63.

[57] Adama S, Bogdan M. Assessing consciousness in patients with locked-in syndrome using their EEG. Front Neurosci 2025;19.

[58] Zilio F, Gomez-Pilar J, Chaudhary U, Fogel S, Fomina T, Synofzik M, et al. Altered brain dynamics index levels of arousal in complete locked-in syndrome. Commun Biol 2023;6(1):1–19.

[59] Kübler A. The history of BCI: From a vision for the future to real support for personhood in people with locked-in syndrome. Neuroethics 2020;13(2):163–80.